SCIENTIFIC REPORTS

OPEN

SUBJECT AREAS:
PETROLOGY
GEOCHEMISTRY
MINERALOGY
VOLCANOLOGY

Received
20 February 2013

Accepted
28 March 2013

Published
10 April 2013

Correspondence and requests for materials should be addressed to V.R.T. (valentin.troll@geo.uu.se)

Magmatic origin of giant 'Kiruna-type' apatite-iron-oxide ores in Central Sweden

Erik Jonsson[1,2], Valentin R. Troll[1], Karin Högdahl[1], Chris Harris[3], Franz Weis[1], Katarina P. Nilsson[2] & Alasdair Skelton[4]

[1]Department of Earth Sciences, CEMPEG, Uppsala University, Villavägen 16, SE-752 36 Uppsala, Sweden, [2]Geological Survey of Sweden, Box 670, Villavägen 18, SE-751 28 Uppsala, Sweden, [3]Department of Geological Sciences, University of Cape Town, 13 University Avenue, Rondebosch 7701, South Africa, [4]Department of Geological Sciences, Stockholm University, Svante Arrhenius Väg 8, SE-106 91 Stockholm, Sweden.

Iron is the most important metal for modern industry and Sweden is by far the largest iron-producer in Europe, yet the genesis of Sweden's main iron-source, the 'Kiruna-type' apatite-iron-oxide ores, remains enigmatic. We show that magnetites from the largest central Swedish 'Kiruna-type' deposit at Grängesberg have $\delta^{18}O$ values between −0.4 and +3.7‰, while the 1.90−1.88 Ga meta-volcanic host rocks have $\delta^{18}O$ values between +4.9 and +9‰. Over 90% of the magnetite data are consistent with direct precipitation from intermediate to felsic magmas or magmatic fluids at high-temperature ($\delta^{18}O_{mgt} > +0.9$‰, i.e. ortho-magmatic). A smaller group of magnetites ($\delta^{18}O_{mgt} \leq +0.9$‰), in turn, equilibrated with high-$\delta^{18}O$, likely meteoric, hydrothermal fluids at low temperatures. The central Swedish 'Kiruna-type' ores thus formed dominantly through magmatic iron-oxide precipitation within a larger volcanic superstructure, while local hydrothermal activity resulted from low-temperature fluid circulation in the shallower parts of this system.

Sweden is by far the biggest producer of iron in Europe[1,2] and iron ore has traditionally been sourced from two principal regions, the Kiruna-Malmberget province in northern Sweden and the Bergslagen region in central Sweden[3] (**Fig. 1**). The apatite-iron-oxide ores of the Grängesberg Mining District (GMD) represents the largest iron ore accumulation in the classic Bergslagen ore province[4], with a past production of 156 Mt of ore, averaging 60% Fe and 0.81% P. Besides iron, phosphates such as fluorapatite and REE-silicates constitute an economically significant reserve of REE[5]. The apatite-iron-oxide deposits of the GMD and its northern continuation are classified to be of 'Kiruna-type', whereas thousands of smaller, but still significant, iron-oxide deposits of banded-iron and skarn-iron types also occur in the Bergslagen province[4,6]. The GMD deposits themselves, are thus traditionally grouped together with those of the Kiruna-Malmberget region[6–8] (i.e., the type locality of the internationally renowned but genetically ambiguous 'Kiruna-type' ores). The origin of this ore-type has been a matter of substantial debate for over 100 years, and several fundamentally different modes of formation have been suggested. These include direct magmatic segregation or crystallization, magmatic hydrothermal replacement, and hydrothermal precipitation in the sense of iron-oxide-copper-gold (IOCG-type) deposits[9–15]. Here we address the primary question, using oxygen isotopes, whether the GMD iron oxides formed through direct magmatic precipitation from either a magma or from high-temperature magmatic fluids (≥ 800°C), likely leading to intrusive-style, massive iron ores, or whether they formed through precipitation from aqueous hydrothermal fluids at lower temperatures (e.g., ≤ 400°C), that would likely form disseminations and vein-type magnetites.

Host rocks to the GMD ores comprise mainly intermediate to felsic meta-volcanic rocks that formed between ~1.90 and 1.88 Ga in a subduction- or back-arc-related tectonic setting[4]. Both the apatite-iron-oxide ores and the meta-volcanic host rocks have been affected by later ductile deformation and the 1.85 to 1.80 Ga Svecokarelian low- to medium-grade metamorphism[4,5]. The exact timing of ore formation in the GMD is not known, but a major regionally-deformed granite body (> 1.85 Ga) occurs directly east of the main Grängesberg ore field and post-dates the ores (**Fig. 1**), because it carries characteristic metre-sized xenoliths of apatite-iron-oxide mineralization. In most parts of the Bergslagen ore province, the host rocks to the ores are SiO_2-rich dacites to rhyolites. In contrast, the host rocks to the GMD ores exhibit more intermediate compositions with a dominance of

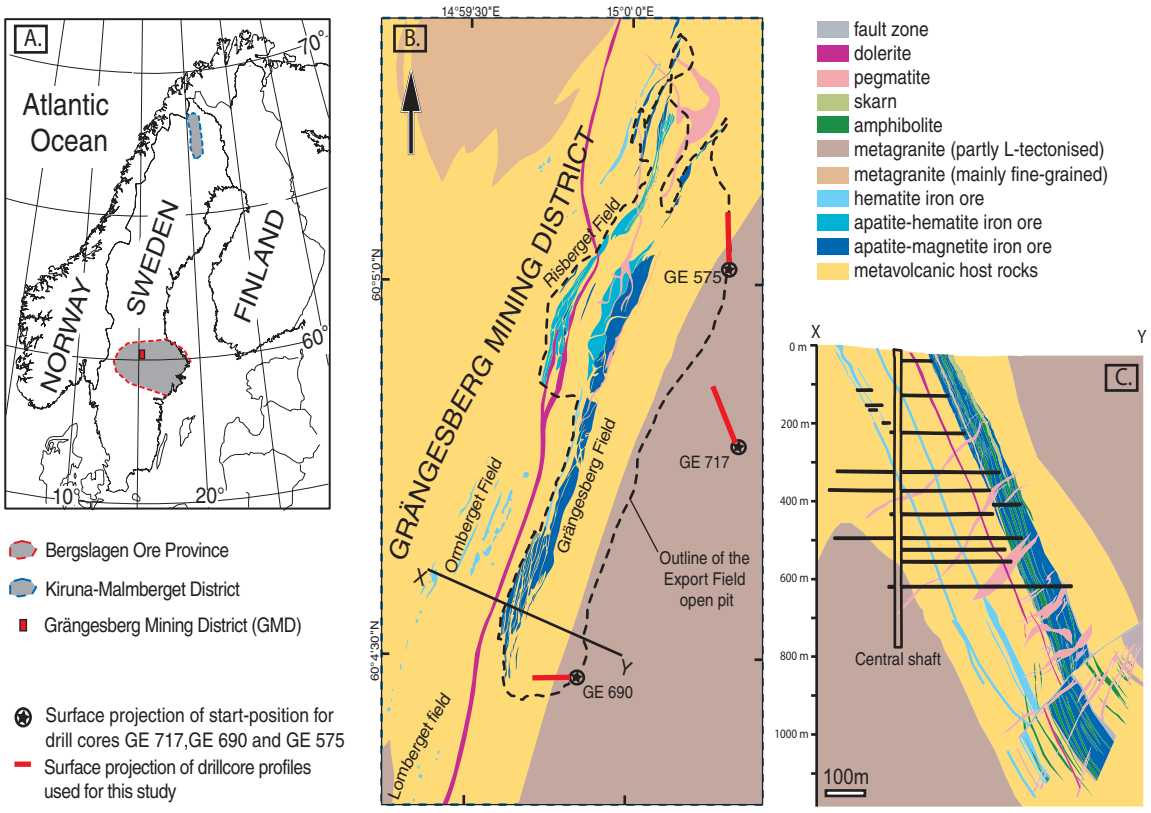

Figure 1 | (A). Overview map of Fennoscandia with the Grängesberg mining district (GMD), the Bergslagen province, and the Kiruna-Malmberget mining district indicated. (B). Geological map over the main ore zone in the GMD. (C). Vertical section (line X–Y in panel B) through the main ore body of the GMD. The ore zone extends downwards at a 70–80° dip to the SE. Black horizontal lines are adits. Modified from Geological Survey of Sweden (SGU) datasets and A. Hallberg, SGU.

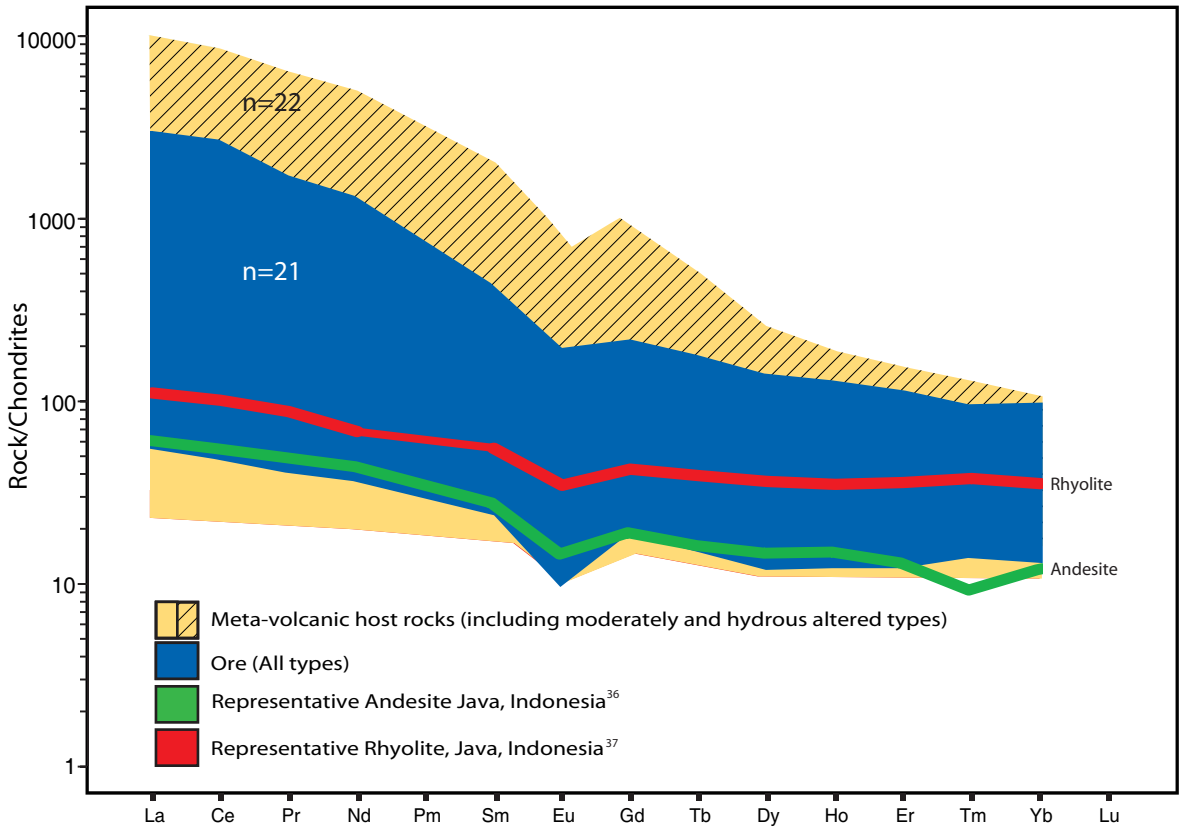

Figure 2 | **Chondrite-normalised REE diagram of host rocks and iron-oxide ores from drill cores 717 and 690.** Chondrite values for normalisation after Sun & McDonough[33]. The iron-oxide ores and the moderately altered host rocks share similar REE concentrations and patterns with the regional bedrock and recent subduction zone volcanic rocks. The hydrous altered host rocks (marked with hatched pattern), in turn, are enriched in REE relative to moderately altered host rocks and recent subduction zone volcanic rocks[36,37].

Table 1 | Grängesberg oxygen isotope data, including sample position along the drillcore profile

Sample	Meters along drillcore (m)	Sample description	Whole Rock $\delta^{18}O$ (‰)	Quartz $\delta^{18}O$ (‰)	Magnetite $\delta^{18}O$ (‰)
Drillcore 690					
KES090003	7.8	Volcanic host rock (meta-dacite)	6.2	7.4	—
KES090004	11.5	Volcanic host rock with hydrous alteration assemblage	7.0	—	—
KES090007	23.6	Volcanic host rock (meta-dacite)	5.2	—	—
KES09008A	23.6	Massive magnetite ore	—	—	1.9
KES090009	29.5	Massive magnetite ore	6.0	—	2.2
KES090011	31.4	Massive magnetite ore	—	—	2.8
KES090012	26.1	Massive magnetite ore	—	—	1.2
KES090014A	32.2	Volcanic host rock (meta-rhyolite)	9.0	—	—
KES090020	55.5	Massive magnetite ore	—	—	1.1
KES090024	63.7	Massive magnetite ore	—	—	1.0
KES 090027	78.7	Massive magnetite ore	—	—	1.2
KES090030	88.8	Massive magnetite ore	—	—	1.8
KES090037	120.4	Massive magnetite ore	—	—	1.4
KES090039	122.4	Volcanic host rock with hydrous alteration assemblage	—	—	3.7
KES090040	123.7	Volcanic host rock with hydrous alteration assemblage	5.5	—	—
KES090044	141.1	Volcanic host rock (meta-andesite)	6.1	—	−0.4
KES090045	139.5	Volcanic host rock with hydrous alteration assemblage	6.5	—	—
Drillcore 717					
KES090048	33.8	Volcanic host rock with hydrous alteration assemblage	6.9	8.0	—
KES090054	55.9	Volcanic host rock with hydrous alteration assemblage	7.1	—	—
KES090056	59.8	Volcanic host rock (meta-dacite)	6.9	—	—
KES090059	84.3	Volcanic host rock (meta-dacite)	6.6	—	—
KES090061	117.3	Volcanic host rock with hydrous alteration assemblage	6.2	—	—
KES090065	147.9	Volcanic host rock with magnetite veins	4.9	5.8	1.3
Grängesberg oxygen isotope data, including sample position along the drillcore profile					
KES090068	167.5	Massive magnetite ore	—	—	1.2
KES090069	167.8	Massive magnetite ore	1.4	—	3.0
KES090070	175.2	Massive magnetite ore	—	—	1.8
KES090071	180.7	Massive magnetite ore	—	—	1.9
KES090072	185.4	Massive magnetite ore	—	—	0.9
KES090073	188.1	Massive magnetite ore	1.3	—	—
KES090077	192.7	Massive hematite ore with disseminated magnetite	—	—	0.2
KES090080	196.2	Massive hematite ore with disseminated magnetite	1.6	—	1.1
KES090081	198.1	Volcanic host rock with hydrous alteration assemblage	—	—	1.5
KES090083B	204.2	Volcanic host rock with hydrous alteration assemblage and magnetite bands	—	—	2.8
KES090086	208.3	Volcanic host rock with magnetite bands	—	—	1.7
KES090087	208.7	Volcanic host rock (meta-dacite) with disseminated magnetite	7.1	6.0	—
KES090088	215.5	Volcanic host rock with hydrous alteration assemblage and magnetite bands	5.6	—	3.4
KES090089	220.9	Volcanic host rock (meta-dacite)	7.0	—	—
Drillcore 575					
KES103011	89.0	Massive magnetite ore	—	—	1.8
KES103016	170.0	Massive magnetite ore	—	—	1.5
Surface Samples					
KH090012	—	Volcanic host rock (meta-dacite)	7.0	6.7	—
KPN090033B	—	Volcanic host rock (meta-andesite)	5.6	6.2	—
KPN090026-4	—	Volcanic host rock (meta-dacite)	6.8	9.1	—
KH09005Ba	—	Volcanic host rock (meta-dacite), magnetite-rich	5.8	7.1	—
KPN090042A	—	Volcanic host rock (meta-dacite)	7.5	6.0	—
KH09005	—	Volcanic host rock (meta-dacite)	5.8	7.0	—
KPN090033A	—	Volcanic host rock (meta-dacite)	8.6	10.3	—

Rock names are based on petrology.

andesites and dacites. The major ore body itself consists of several lenses that occur along a planar NNE-trending zone with a moderate to steep eastward dip. The principal orientation of the major ore body is stratiform, i.e. it is parallel to the internal contacts within the meta-volcanic host rocks that themselves are sub-parallel to the main tectonic trend in the region. Magnetite occurs either in massive ore lenses or as veins, bands or disseminations (hereafter referred to as VeDi-magnetites). Within the central part of the GMD ore field, a number of dykes and sills exhibit cross-cutting relationships to rock units of similar composition, on which basis we interpret the

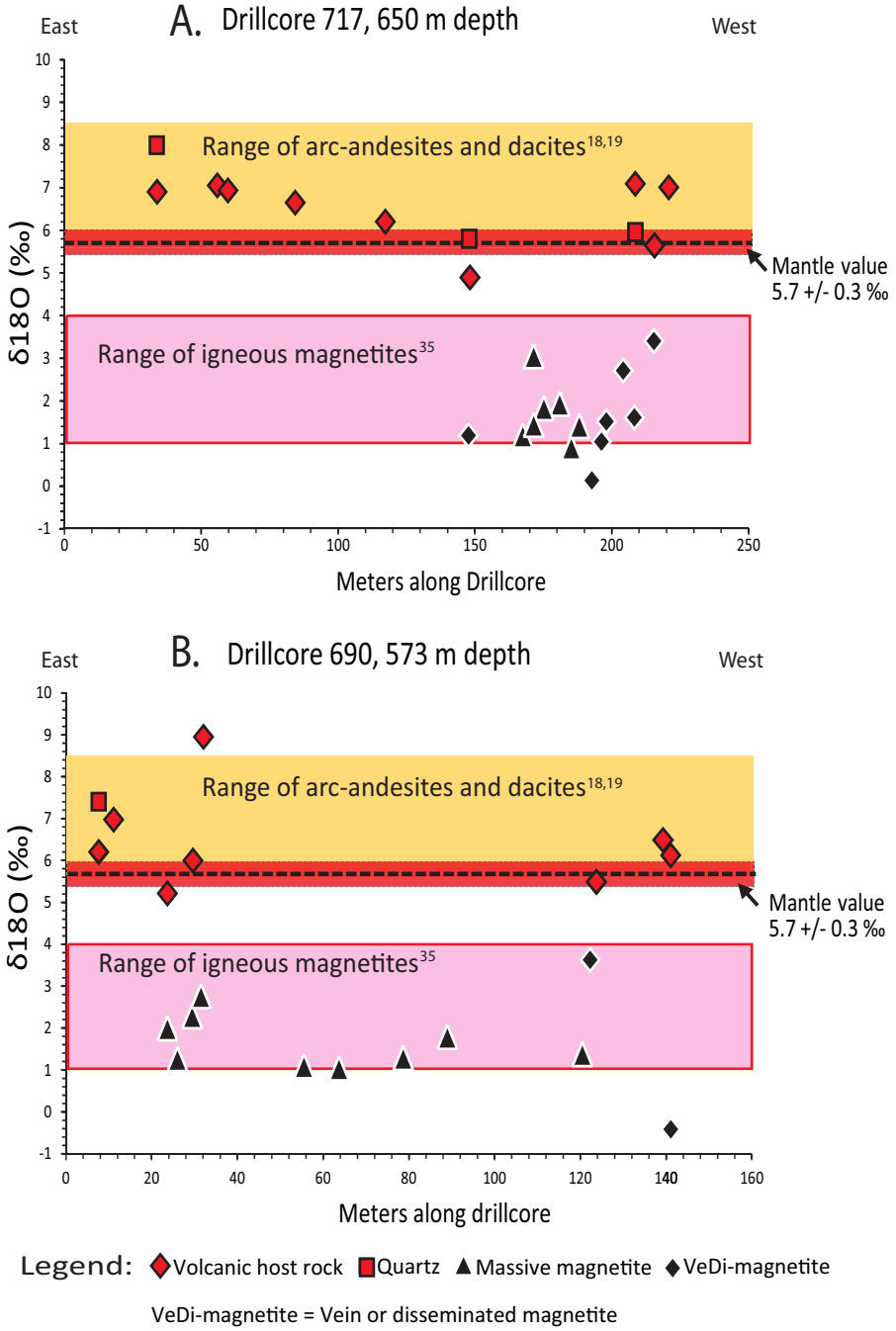

Figure 3 | Parts (A) and (B) show the oxygen isotope data for two drill cores (Numbers 690 and 717) that traverse the main ore zone at Grängesberg between 570 and 670 m below the surface (see Fig. 1). Shown are the oxygen isotope compositions of the host rocks, quartz separates, massive magnetites and VeDi-magnetites, the latter including magnetite from hematite ore. All oxygen data are reported in standard $\delta^{18}O$-notation relative to SMOW after Hoefs[34]. The $\delta^{18}O$ ranges for the mantle and arc-andesites are after Bindemann[18] and Taylor[19]. Range of igneous magnetites after Taylor[35].

emplacement environment as "shallow sub-volcanic" in character. Hydrous alteration is evident in the direct host rocks to the ore in the form of disseminated and sometimes discrete biotite, chlorite or variably amphibole- and fluorapatite-rich assemblages. Massive magnetite ores seem unaffected by this alteration or by the regional metamorphism. However, the hydrous alteration assemblages are always spacially related with the massive ore and are absent beyond the main ore zone, implying a genetic relationship between the two.

Results

Samples were collected from surface exposures and from three shallow plunging ($\leq 20^{\circ}$) drill cores that transect the steeply dipping ore body between −570 and −670 m (**Fig. 1**). The GMD apatite-iron-oxide ore is either magnetite- or hematite-dominated, and is variably enriched in fluorapatite and accessory silicate phases (amphiboles, biotite, chlorite *sensu lato*) and REE-minerals. Most ore-types show some degree of banding, defined by aggregates of mostly fine-grained fluorapatite and minor amounts of silicates. The main GMD ore field, locally known as the 'Export Field', is estimated to consist of about 80% magnetite and 20% hematite ore, with a concentration of the latter near the structural footwall.

In addition to fluorapatite, REEs are hosted in associated monazite-(Ce), allanite-(Ce), xenotime-(Y), LREE-bearing epidote, and REE fluorocarbonates. Although the GMD apatite-iron-oxide ores

Table 2 | Calculated oxygen isotopic compositions for magmas and fluids in equilibrium with magnetite samples

Magnetite Sample	Magnetite $\delta^{18}O$ (‰)	Theoretical magma $\delta^{18}O$ (‰) for fractionation from andesite	Value fit	Theoretical magma $\delta^{18}O$ (‰) for fractionation from dacite	Value fit	Theoretical aqueous ore fluid $\delta^{18}O$ (‰) for fractionation from high-T fluid	Value fit
KES090081	1.5	5.5	x	5.8	✓	6.7	✓
KES090083B	2.8	6.8	✓	7.1	✓	8.0	✓
KES090088	3.4	7.4	✓	7.7	✓	8.6	✓
KES090069	3.0	7.0	✓	7.3	✓	8.2	✓
KES090071	1.9	5.9	✓	6.2	✓	7.1	✓
KES090086	1.7	5.7	✓	6.0	✓	6.9	✓
KES09008A	1.9	5.9	✓	6.2	✓	7.1	✓
KES090009	2.2	6.2	✓	6.5	✓	7.4	✓
KES090037	1.4	5.4	x	5.7	✓	6.6	✓
KES090039	3.7	7.7	✓	7.9	✓	8.9	✓
KES090044	−0.4	3.6	x	3.9	x	4.8	x
KES090065	1.3	5.3	x	5.6	x	6.5	✓
KES090077	0.2	4.2	x	4.5	x	5.4	x
KES090080	1.1	5.0	x	5.4	x	6.3	✓
KES090011	2.8	6.7	✓	7.1	✓	8.0	✓
KES090030	1.8	5.8	✓	6.1	✓	7.0	✓
KES090012	1.2	5.2	x	5.5	x	6.4	✓
KES090020	1.1	5.0	x	5.4	x	6.3	✓
KES090027	1.2	5.2	x	5.5	x	6.4	✓
KES090072	0.9	4.8	x	5.2	x	6.1	✓
KES090024	1.0	5.0	x	5.3	x	6.2	✓
KES090068	1.2	5.1	x	5.5	x	6.4	✓
KES090070	1.8	5.8	✓	6.1	✓	7.0	✓
KES103011	1.8	5.8	✓	6.1	✓	7.0	✓
KES103016	1.5	5.5	x	5.8	✓	6.7	✓

1. $1000\ln\alpha_{(mt-andesite)} = -4.0$ ‰, $1000\ln\alpha_{(mt-dacite)} = -4.3$ ‰, regular range of arc andesites/dacites 5.7 – 8 ‰[18].
2. $1000\ln\alpha_{(mt-water\ 800^{\circ}C)} = -5.2$ ‰ , regular range for magmatic waters 6–8‰[20,34].
✓ = in equilibrium with magma/magmatic water ; X= not in equilibrium with common magmatic values.

are typically enriched in Th, U, La, Ce, Nd, P, Fe, Sm, Tb, Y, Tm and Yb, they are depleted in K, Ba, Sr, Zr and Ti relative to average continental crust. The ores themselves, and particularly the apatite-rich samples and the hydrous host rock alteration assemblages, display negative Eu-anomalies and flat HREE patterns. The hydrous altered host rocks and the apatite-rich assemblages associated with the ore show the same REE enrichment patterns as moderately altered host rocks, but are elevated by several orders of magnitude when compared with the meta-volcanic rocks in the region and with typical subduction zone andesites and rhyolites (**Fig. 2**).

To distinguish between magmatic and magmatic-hydrothermal origins of magnetite, which together we term "ortho-magmatic", is not possible with our data. However, a low-temperature hydrothermal origin ($\leq 400^{\circ}C$) versus a high-T ortho-magmatic origin can be discerned. Oxygen isotope ratios have been measured on 63 samples of meta-volcanic host rocks, hydrous alteration-assemblages, quartz mineral separates, as well as magnetite from massive ore, veins, and disseminations, and from hematite-dominated ore. All data are reported in delta notation relative to SMOW (**Table 1**). The host rock $\delta^{18}O$ values, including whole rocks and quartz mineral separates from both outcrops and drill cores, range from +4.9 to +10.3‰, i.e. within the spectrum of most normal igneous rock compositions. The massive iron-ores from the main ore body yield $\delta^{18}O$ values, between +0.9 and +3.0‰ [n = 16] (**Fig. 3**). The $\delta^{18}O$ values of all GMD magnetite samples, including vein and disseminated magnetite types [n = 7] as well as magnetite inclusions in hematite ore [n = 2] range from −0.4 to +3.7‰. The origin of the different magnetite types can be assessed using O-isotope fractionation between magnetites and an andesitic parent magma at magmatic temperatures ($\geq 900^{\circ}C$) ($\Delta_{magnetite-andesite} = -4.0$‰) or with magmatic water ($\Delta_{magnetite-water} = -5.2$‰ at $800^{\circ}C$)[16,17]. Magnetites with $\delta^{18}O \geq +1.7$‰ yield equilibrium magma values between +5.7 and +7.7‰ (**Table 2**), i.e. within the range of subduction zone andesite magmas (+5.7 to +8.5‰)[18,19]. Using the fractionation factor for magnetite from a dacite magma ($\Delta_{magnetite-dacite} = -4.3$‰)[17], the theoretical magma values would shift upwards by +0.3‰, moving them further into the intermediate magmatic range that is characteristic for continental subduction zone rocks[18,19] (**Figs. 3, 4, Table 2**). These results are compatible with our andesite to dacite host rock data that range between +4.9 and +9.0‰ (**Table 1**). In turn, magnetite samples with $\delta^{18}O$ values $\geq$ +0.9‰ satisfy equilibrium conditions with high-temperature magmatic waters of +6.1 to +8.9‰ (**Table 2**), which corresponds to the range of common magmatic waters (6–8‰)[20]. Thus, all GMD magnetites with $\delta^{18}O$ values $\geq$ +0.9‰ (> 90% of our samples) are consistent with an 'ortho-magmatic' mode of formation because they satisfy high-temperature magmatic equilibrium conditions (pale pink box in **Fig. 4**). Notably, this field hosts all GMD massive magnetite ore samples, as well as several VeDi samples. Magnetites with $\delta^{18}O$ values below +0.9‰, in turn, cannot be in equilibrium with a regular magma or with a high-temperature magmatic fluid, but must have formed from a high-$\delta^{18}O$ hydrothermal fluid at more moderate temperatures. Low-temperature processes increase mineral-fluid fractionation, i.e. fractionation factors become more negative (e.g. $\Delta_{magnetite-water} \leq -7.6$‰ at $T \leq 400^{\circ}C$)[16], implying oxygen isotope exchange at low temperatures for the magnetites $\leq$ 0.9‰. A high-$\delta^{18}O$ hydrothermal fluid from the uppermost range of meteoric fluids[21], or a mix of remnant magmatic water and a meteoric influx, can explain the remaining VeDi magnetites (n = 2), while satisfying the low-temperature fractionation conditions (**Fig. 4**).

Employing a similar approach on host rock quartz, a mineral that is assumed to be resistant to oxygen isotope resetting once formed, should allow us to test the results derived from the magnetite data. Quartzes have $\delta^{18}O$ values between +5.8 and +10.3‰

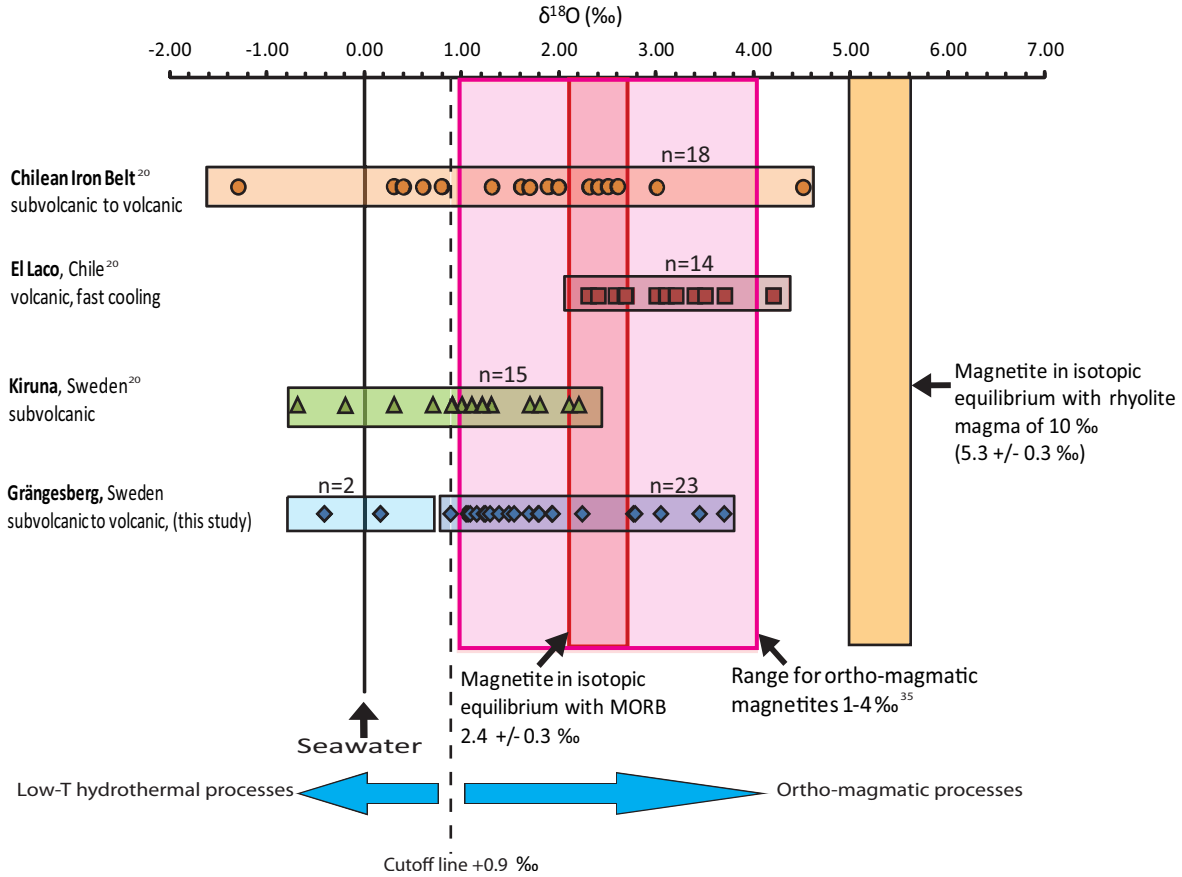

Figure 4 | Magnetite $\delta^{18}O$ values from GMD compared to other volcanically-hosted iron ore deposits. For reference, magnetites in equilibrium with MORB [red box], the range for typical 'ortho-magmatic' magnetites after Taylor[35] [pale pink box] and magnetite in equilibrium with an evolved rhyolite with a $\delta^{18}O$ of 10‰ (the demarcation between I-type (<10‰) and S-type (>10‰) magmas) are shown. The GMD magnetites plot dominantly above the +0.9‰ demarcation and in the field of 'ortho-magmatic' magnetites after Taylor[35]), and satisfy equilibrium with magma or magmatic fluids at magmatic temperatures (~800–1000°C). A small fraction of the GMD data (n = 2), however, is more consistent with formation from a low-temperature fluid regime. The cut-off point for this is calculated to be +0.9‰ in magnetites, because fractionation factors determine that samples < +0.9‰ cannot be in equilibrium with either a magma or a magmatic fluid at high temperatures (≥ 800°C). Magnetites with values lower than +0.9‰ are calculated to have been in equilibrium with a high- $\delta^{18}O$ (likely meteoric) fluid at temperatures of ≤400°C.

(n = 11, **Table 3**). Taking $\Delta_{qtz-magma}$ = +0.9‰ and +0.8‰[17] as fractionation between quartz and andesite and quartz and dacite magmas respectively, $\delta^{18}O$ melt values of +4.9 to +9.5‰ are derived (n = 22, **Table 3**). Seven out of 11 quartz $\delta^{18}O$ values correspond to calculated magmatic values for andesites and dacites with $\delta^{18}O \geq +5.7‰$[18]. A calculated fractionation temperature for a co-existing quartz and magnetite pair for the GMD deposit that appears in textural and oxygen-isotope equilibrium yields a temperature of 907 ± 53°C, consistent with temperatures expected for oxide formation from intermediate to evolved (hydrous) arc magmas and consistent with phase relations and experimental constraints[9,10,13,22]. Quartz with $\delta^{18}O \leq +6.2‰$ (n = 4) would be in equilibrium with a magmatic fluid at temperatures between 800°C and 900°C ($\Delta_{quartz-water}$ = +0.3 to −0.1‰), which implies that these quartzes are of ortho-magmatic origin too (following our initial definition).

Discussion

The relatively wide range of $\delta^{18}O$ in the GMD host rocks (+4.9 to +9.0‰, **Table 1**) suggests that some host rock and VeDi-samples reflect low- and high-temperature alteration processes (e.g. silicate whole rocks with $\delta^{18}O > 8.5‰$ and < 5.7‰ respectively). Massive magnetite ores, in turn, show textural characteristics and $\delta^{18}O$ values that support precipitation from a magma. Those massive magnetites are chemically and mechanically refractory and appear little affected by later overprint (i.e., they were resistant to subsequent exchange with fluids or there were insufficient fluids to exchange with). In addition, the temperature and oxygen isotope data derived for the refractory GMD quartz and magnetite samples fall in the magmatic range also and overlap with those presented in Nyström et al.[20] for the iconic El Laco apatite-iron-oxide deposit in Chile (~700° – 800°C). Discussion is, however, ongoing regarding the genesis of the El Laco deposit, and the possibility of interaction with a high-$\delta^{18}O$ hydrothermal fluid exists because the data for almost all textural magnetite types at El Laco average around +4‰[23]. These authors[23] argue that a 'natural' spread between "magmatic" and "low-temperature hydrothermal" signals would be expected for a truly "magmatic" formation because a large volcano would logically develop an associated hydrothermal system at shallower levels. Although maybe not observed at El Laco, the GMD data show a small group of low-temperature magnetites, making our proposed dominantly ortho-magmatic formation scenario rather probable. The potential wider significance of this result is further underlined by the fact that our GMD data encompass the available $\delta^{18}O$-data from Kiruna[20], the largest apatite-iron-oxide deposit in Europe, suggesting very similar modes of formation for the GMD and Kiruna deposits (**Fig. 4**).

On the basis of the data presented, the massive apatite-iron-oxide ores at GMD formed in equilibrium with mafic to felsic magmas at magmatic temperatures (i.e., probably with subduction-type andesites to dacites, which form the host rocks to the ores in the region).

Table 3 | The results for of the quartz-magma equilibrium fractionation calculation

Sample	Type	Appx. distance from ore body	Description	Whole Rock $\delta^{18}O$ (‰)	Quartz $\delta^{18}O$ (‰)	Theoretical andesite magma $\delta^{18}O$ (‰)	Value fit	Theoretical dacite magma $\delta^{18}O$ (‰)	Value fit
KES090048	Country rock, drillcore	0 m	Volcanic host rock with hydrous alteration assemblage	6.9	8.0	7.1	✓	7.2	✓
KES090065	Ore sample, drillcore	0 m	Volcanic host rock with magnetite veins	4.9	5.8	4.9	X	5.0	X
KES090087	Ore sample, drillcore	0 m	Volcanic host rock with disseminated magnetite	7.1	5.9	5.0	X	5.1	X
KES090003	Country rock, drillcore	0 m	Volcanic host rock (meta-dacite)	6.2	7.4	6.5	✓	6.6	✓
KH090012	Country rock	700 m to S	Volcanic host rock (meta-dacite)	7.0	6.7	5.7	✓	5.8	✓
KPN090033B	Country rock	1000 m to NW	Volcanic host rock (meta-andesite)	5.6	6.2	5.3	X	5.4	X
KPN090026−4	Country rock	1000 m to SW	Volcanic host rock (meta-dacite)	6.8	9.1	8.2	✓	8.3	✓
KH09005Ba	Country rock	1200 m to N	Volcanic host rock (meta-dacite), magnetite-rich	5.8	7.1	6.2	✓	6.3	✓
KPN090042A	Country rock	1400 m to NW	Volcanic host rock (meta-dacite)	7.5	6.0	5.1	X	5.2	X
KH09005	Country rock	1200 m to N	Volcanic host rock (meta-dacite)	5.8	7.0	6.1	✓	6.2	✓
KPN090033A	Country rock	1000 m to NW	Volcanic host rock (meta-dacite)	8.6	10.3	9.4	✓	9.5	✓

✓ = In equilibrium with magmatic values ; X= not in equilibrium with common magmatic values.

The hydrous alteration assemblages, in turn, have highly variable $\delta^{18}O$ values, but their REE patterns are very similar to that of the ores. In combination with their exclusive occurrence close to the ore zone, this observation suggests a genetic relationship between iron-oxide ores and the REE-enrichment in hydrous alteration assemblages[24–26]. Medium- to low-temperature hydrothermal alteration associated with ore formation and emplacement is consistent with a scenario of high-temperature oxide-rich magmas intruding an upper crustal volcano-sedimentary pile where they initiate fluid circulation at more moderate temperatures. At GMD, volcaniclastic host rocks are locally extensively brecciated as well as crosscut by dykes and other sheet intrusions, which in combination with our REE and oxygen isotope data supports a shallow-level sub-volcanic environment. The VeDi-type magnetites and hydrous alteration assemblages formed in proximity to the massive ore bodies, and a degree of overlap between these regimes (i.e., high-temperature ortho-magmatic versus low-temperature hydrothermal), is expected for a sub-volcanic mode of formation[23]. Our preferred interpretation is therefore that of a now deformed, originally large and possibly of caldera-type[4], volcanic complex situated in a subduction zone regime. Ascent, intrusion, and crystallization of oxide-rich melts to shallow levels within the volcanic plumbing system produced dominantly ortho-magmatic magnetite, while low-temperature hydrothermal activity near the surface occured to some extent. This late hydrothermal activity likely involved exsolved magmatic volatiles as well as external meteoric waters that probably became available to the host system at shallower levels and at progressively lower temperatures[23,27]. This realisation helps us to better understand the formation of Europe's most important iron source, the 'Kiruna-type' apatite-iron oxide ores of central and northern Sweden.

Methods

REE analysis. A total of 44 drill core samples including both, moderately to intensely and hydrous altered host rocks (9 and 15 samples, respectively) and sections from the iron oxide ore (20 samples) were analysed for Rare Earth Elements (REE) at *Acme Analytical Labs Ltd* in Vancouver, Canada. Trace and rare earth elements were analysed by inductively coupled plasma-mass spectrometry (ICP-MS) after preparation by multi-acid digestion. Loss on ignition (i.e. volatile content) was determined by igniting a sample split and then measuring weight loss. Data quality was monitored using a set of certified, internal reference materials. Detailed information on uncertainties and reproducibility can be found at http://acmelab.com/services/method-descriptions/soil-till-and-sediment/.

Oxygen Isotopes. All O-isotope data presented in this paper were produced at the University of Cape Town (UCT). For oxygen isotopes, both conventional and laser fluorination methods were used. Some quartz, and all magnetite, separates were analysed using a conventional silicate line (described in **Harris & Ashwal**[28]). Approximately 20 mg (magnetite) and 10 mg (quartz) of sample was reacted with ClF_3, and the liberated O_2 converted to CO_2 using a hot platinized carbon rod. Magnetite was reacted overnight at 600°C and all other minerals were reacted for 4 hours at 550°C. Some quartz and magnetite separates were analysed using the laser fluorination analytical process described in **Harris & Vogeli**[29]. Each sample was reacted in the presence of approximately 10 kPa BrF_5 and the purified O_2 was collected onto a 5Å molecular sieve contained in a glass storage bottle.

All isotope ratios were measured off-line using a Finnigan Delta XP mass spectrometer in dual-inlet mode. All data are reported in δ notation where $\delta^{18}O = (R_{sample}/R_{standard} - 1)*1000$, and R = the measured ratio (i.e.$^{18}O/^{16}O$ or D/H). Duplicate splits of the quartz standard (NBS28) run with each batch of eight samples were used to convert the raw data to the SMOW scale using the $\delta^{18}O$ value of 9.6‰ for NBS28 recommended by **Coplen et al.**[30]. During the course of this work, 8 analyses of NBS28 gave a 2σ error of 0.2. The O-isotope ratios of samples analysed using laser fluorination were measured on O_2 gas. Measured values of our internal standard MON GT[31] were used to normalise raw data and correct for drift in the reference gas. The average difference in $\delta^{18}O$ values of duplicates of MON GT analysed during this study was 0.1‰, and corresponds to a 2σ value of 0.2‰. MON GT was recalibrated against the UWG-2 garnet standard of **Valley et al.**[32] using the current laser system, and has a revised $\delta^{18}O$ value of 5.4‰, assuming a $\delta^{18}O$ value of 5.8‰ for UWG2.

1. Vaughan, D. J. The mastery of iron. *Elements* **7**, 75 (2011).
2. U.S. Geological Survey. Mineral commodity summaries 2011. *U.S. Geological Survey*, 198 p. (2011).

3. Williams, P. J. *et al.* Iron oxide copper-gold deposits: geology, space-time distribution, and possible modes of origin. *Economic Geology* **100**, 371–405 (2005).
4. Allen, R. L., Lundström, I., Ripa, M., Simeonov, A. & Christofferson, H. Facies analysis of a 1.9 Ga, continental margin, back-arc felsic caldera province with diverse Zn-Pb-Ag-(Cu-Au) sulphide and Fe oxide deposits, Bergslagen region, Sweden. *Economic Geology* **91**, 979–1008 (1996).
5. Jonsson, E., Nilsson, K. P., Hallberg, A. & Högdahl, K. The Palaeoproterozoic apatite-iron oxide deposits of the Grängesberg area: Kiruna-type deposits in central Sweden. In: Nakrem, H. A., Harstad, A. O. & Haukdal, G. (eds.) *NGF abstracts and proceedings* **1**, 88–89 (2010).
6. Looström, R. Likheter mellan Lapplands- och Grängesbergsmalmerna. *GFF* **51**, 303–308 (1929).
7. Geijer, P. & Magnusson, N. H. (1944) De mellansvenska järnmalmernas geologi. SGU series Ca 35. 654 pp.
8. Hitzman, M. W., Oreskes, N. & Einaudi, M. T. Geologic characteristics and tectonic setting of Proterozoic iron oxide (Cu-U-Au-REE) deposits. *Precambrian Research* **58**, 241–287 (1992).
9. Naslund, H. R. The effect of oxygen fugacity on liquid immiscibility in iron-bearing silicate melts. *American Journal of Science* **283**, 1034–1059 (1983).
10. Weidner, J. R. Iron-oxide magmas in the system Fe-C-O. *Canadian Mineralogist* **20**, 555–566 (1982).
11. Geijer, P. Igneous rocks and iron ores of Kiirunavaara, Luossavaara and Tuolluvaara. Geologie des Kirunagebiets 2, 278 pp. (1910).
12. Parak, T. Kiruna iron ores are not "intrusive-magmatic ores of the Kiruna Type" *Economic Geology* **70**, 1242–1258 (1975).
13. Nyström, J. O. & Henriquez, F. Magmatic features of iron ores of the Kiruna type in Chile and Sweden: Ore textures and magnetite geochemistry. *Economic Geology* **89**, 820–839 (1994).
14. Barton, M. D. & Johnson, D. A. Evaporitic source model for igneous-related Fe oxide (REE-Cu-Au-U) mineralization. *Geology* **24**, 259–262 (1996).
15. Sillitoe, R. H. & Burrows, D. R. New field evidence bearing on the origin of the El Laco magnetitedeposit, northern Chile. *Economic Geology* **97**, 1101–1109 (2002).
16. Zheng, Y. F. Calculation of oxygen isotope fractionation in metal oxides. *Geochimica and Cosmochimica Acta* **55**, 2299–2307 (1991).
17. Zhao, Z. F. & Zheng, Y. F. Calculation of oxygen isotope fractionation in magmatic rocks. *Chemical Geology* **193**, 59–80 (2003).
18. Bindeman, I. Oxygen isotopes in mantle and crustal magmas as revealed by single crystal analysis. *Reviews in Mineralogy & Geochemistry* **69**, 445–478 (2008).
19. Taylor, H. P. The oxygen isotope geochemistry of igneous rocks. *Contributions to Mineralogy and Petrology* **19**, 1–71 (1968).
20. Nyström, J. O., Billström, K., Henríquez, F., Fallick, A. E. & Naslund, H. R. Oxygen isotope composition of magnetite in iron ores of the Kiruna type in Chile and Sweden. *GFF* **130**, 177–188 (2008).
21. Craig, H. Isotopic variations in meteoric waters. *Science* **133**, 1702–1703 (1961).
22. Kolker, A. Mineralogy and geochemistry of Fe-Ti oxide and apatite (Nelsonite) deposits and evaluation of the liquid immiscibility hypothesis. *Economic Geology* **77**, 1146–1158 (1982).
23. Rhodes, A. L. & Oreskes, N. Oxygen isotope composition of magnetite deposits at El Laco, Chile: Evidence of formation from isotopically heavy fluids. In: Skinner, B. J. (ed) *Economic Geology Special Publication* **7**, 333–351 (1999).
24. Jochum, K. P. & Verma, S. P. Extreme enrichment of Sb, Tl and other trace elements in altered MORB. *Chemical Geology* **130**, 289–299 (1996).
25. Hill, I. G., Worden, R. H. & Meighan, I. G. Yttrium: The immobility-mobility transition during basaltic weathering. *Geology* **28**, 923–926 (2000).
26. Williams-Jones, A. E., Migdisov, A. A. & Samson, I. M. Hydrothermal mobilisation of the rare earth elements: a tale of "Ceria" and "Yttria". *Elements* **8**, 355–360 (2012).
27. Donoghue, E., Troll, V. R. & Harris, C. Hydrothermal alteration of the Miocene Tejeda Intrusive Complex, Gran Canaria, Canary Islands: insights from petrography, mineralogy and O− and H− isotope geochemistry. *Journal of Petrology* **51**, 2149–2176 (2010).
28. Harris, C. & Ashwal, L. D. The origin of low δ^{18} O granites and related rocks from the Seychelles. *Contributions to Mineralogy and Petrology* **143**, 366–376 (2002).
29. Harris, C. & Vogeli, J. Oxygen isotope composition of garnet in the Peninsula Granite, Cape Granite Suite, South Africa: constraints on melting and emplacement mechanisms. *South African Journal of Geology* **113**, 401–412 (2010).
30. Coplen, T. B., Kendall, C. & Hopple, J. Intercomparison of stable isotope reference samples. *Nature* **302**, 236–238 (1983).
31. Harris, C., Smith, H. S. & le Roex, A. P. Oxygen isotope composition of phenocrysts from Tristan da Cunha and Gough Island lavas: Variation with fractional crystallization and evidence for assimilation. *Contributions to Mineralogy and Petrology* **138**, 164–175 (2000).
32. Valley, J. W., Kitchen, N., Kohn, M. J., Niendorf, C. R. & Spicuzza, M. J. UWG-2, a garnet standard for oxygen isotope ratios: Strategies for high precision and accuracy with laser heating. *Geochim. Cosmochim. Acta* **59**, 5223–5231 (1995).
33. Sun, S. S. & McDonough, W. F. Chemical and isotopic systematics of ocean basalts: implications for mantle composition and processes. In: Saunders, A. D. & Norry, M. J. (eds.) Magmatism in ocean basins. *Geological Society of London Special Publication* **42**, 313–345 (1989).
34. Hoefs, J. *Stable Isotope Geochemistry* (Springer-Verlag, Berlin, Heidelberg, New York, 1997).
35. Taylor, H. P. Oxygen isotope studies of hydrothermal mineral deposits. In: Barnes, H. L. (ed.): *Geochemistry of Hydrothermal Ore Deposits* pp.109–142 (Holt, Rinehart and Winston Inc., New York, 1967).
36. Handley, H. K., Macpherson, C. G., Davidson, J. P., Berlo, K. & Lowry, D. Constraining fluid and sediment contributions to subduction-related magmatism in Indonesia: Ijenvolcanic complex. *Journal of Petrology* **48**, 1155–1183 (2007).
37. Gardner, M. F. *et al.* Crustal differentiation processes at Krakatau volcano, Indonesia. *Journal of Petrology*, doi:10.1093/petrology/egs066, 1–34 (2012).

Acknowledgements

We thank the Geological Survey of Sweden (SGU) for access to the GMD drillcores and Fayrooza Rawoot is thanked for help with the O-isotope analyses at Cape Town University. This work is funded by the Geological Survey of Sweden (SGU), the Swedish Research Council (VR), and the National Research Foundation of South Africa.

Author contributions

The project was jointly conceived by E.J., V.R.T., K.H. and K.P.N. Analyses and data interpretation were carried out by E.J., V.R.T., C.H., F.W., K.H. and A.S. and writing was done by all authors working on a draft by E.J., V.R.T. and K.H.; E.J. and V.R.T. contributed in approximately equal proportions.

Additional information

Competing financial interests: The authors declare no competing financial interests.

How to cite this article: Jonsson, E. *et al.* Magmatic origin of giant 'Kiruna-type' apatite-iron-oxide ores in Central Sweden. *Sci. Rep.* **3**, 1644; DOI:10.1038/srep01644 (2013).